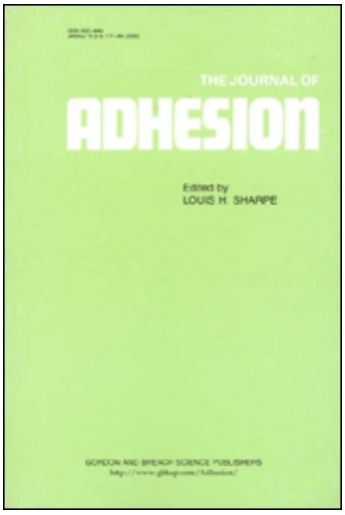

The Journal of Adhesion
Publication details, including instructions for authors and subscription information:
http://www.informaworld.com/smpp/title~content=t713453635

Bulk, Surface, and Interfacial Characterization of Silicone - Polyurea Segmented Copolymers

David J. Kinning[a]
[a] 3M Company, St. Paul, MN, USA

To cite this Article Kinning, David J.(2001) 'Bulk, Surface, and Interfacial Characterization of Silicone - Polyurea Segmented Copolymers', The Journal of Adhesion, 75: 1, 1 — 26
To link to this Article: DOI: 10.1080/00218460108029591
URL: http://dx.doi.org/10.1080/00218460108029591

J. Adhesion, 2001, Vol. 75, pp. 1 - 26
Reprints available directly from the publisher
Photocopying permitted by license only

Bulk, Surface, and Interfacial Characterization of Silicone – Polyurea Segmented Copolymers*

DAVID J. KINNING†

3M Company, St. Paul, MN 55144, USA

(Received 26 February 2000; In final form 4 May 2000)

In this paper the bulk, surface and interfacial structures of a series of polyureas containing polydimethylsiloxane segments are examined. The silicone polyureas studied here all contain 25 wt% of a 5,000 molecular weight aminopropyl-terminated polydimethylsiloxane diamine, along with various ratios of a 900 molecular weight polypropylene oxide diamine soft segment and hard segments comprised of isophorone diisocyanate and 1,3 diamino pentane chain extender. The bulk morphology and rheology of the silicone polyureas are studied using transmission electron microscopy, differential scanning calorimetry, and dynamic mechanical thermal analysis. The siloxane segments are observed to form well-phase-separated spherical microdomains, while the matrix phase is comprised of a mixture of the polypropylene oxide soft segments and the hard segments. The single glass transition temperature of the matrix phase increases systematically as the ratio of hard segment to polypropylene oxide soft segment increases. The surfaces of the silicone polyureas are characterized using contact angle analysis, X-ray photoelectron spectroscopy and static secondary ion mass spectrometry. All of the silicone polyureas exhibit a thin 15 to 20 Å overlayer of the siloxane segments at their surface. The ability of the silicone polyurea surfaces to restructure upon contact with either water or an acid-functional acrylate pressure sensitive adhesive is also studied. The extent and rate of decrease in the receding water contact angle, as a function of water dwell time and temperature, are related to the segmental mobility within the near-surface region of the silicone polyurea coatings. Silicone polyureas having higher hard segment content, and higher non-silicone matrix glass transition temperatures, are better able to maintain a high water receding contact angle, due to their lower segmental mobility. The observed increases in adhesion of the pressure sensitive adhesive, with increasing aging time and/or temperature, are attributed to an increase in the acid-base interactions between urea groups in the silicone polyurea and acrylic acid groups in the PSA. The initially low peel forces can be more readily

* Presented at the Nineteenth Annual Meeting of the Adhesion Society, Inc., Myrtle Beach, South Carolina, USA, February 18 - 21, 1996.

† Tel.: 651-736-8282, Fax: 651-737-4682, e-mail: djkinning1@mmm.com

maintained for the silicone polyureas having high hard segment contents, due to the reduced segmental mobility and reduced degree of interfacial restructuring within the silicone polyurea.

Keywords: Silicone; Polyurea; Surface; Interfacial restructuring; Adhesion

INTRODUCTION

It is well known that block and segmented type copolymers exhibit an enrichment of the low surface energy component at their surfaces due to the minimization of surface free energy [1 – 10]. It has also been realized that polymeric materials, by their very nature, exhibit some degree of segmental mobility and can restructure upon contact with another medium [11]. Restructuring of polymeric surfaces, driven by the minimization of interfacial energy, has been shown to occur for a number of multicomponent polymeric materials, including hydrogels [12 – 14], oxidized or surface functionalized olefins [13, 15, 16] or fluorocarbon polymers [17, 18], graft or block copolymers [3, 19 – 29], alkyl [30, 31] or fluoroalkyl [32] side chain polymers, polymer networks [33, 34], and polyurethanes [5, 6, 25, 35 – 37]. Such restructuring can lead to changes in the chemical interactions at interfaces and is, therefore, an important phenomenon to consider in applications involving properties such as adhesion, wetting or repellency, biocompatibility, printability, *etc.*

In this paper the bulk, surface and interfacial structures of a series of polyureas containing polydimethylsiloxane segments, and a range of hard segment contents, are examined. The thermal and rheological response of these silicone polyureas is related to their composition, bulk microdomain morphology and the degree of mixing of the different segments. While all of the silicone polyureas show a significant enrichment of the siloxane segments at their surface, they respond quite differently to contact with orienting media. The degree and rate of interfacial restructuring is probed through measurements of contact angles and adhesion of a pressure sensitive adhesive (PSA). The changes in the water receding contact angle and peel adhesion of the pressure sensitive adhesive, with increasing contact time and/or temperature, are related to the segmental mobility within the silicone polyureas.

EXPERIMENTAL METHODS

Synthesis of Silicone Polyureas

The silicone polyureas studied here all contained 25 wt% of a 5,000 molecular weight aminopropyl-terminated polydimethylsiloxane diamine, prepared according to the method described by Hoffman and Leir [38]. In addition, the silicone polyureas contained various amounts of a 900 molecular weight amine-terminated poly(propylene oxide) diamine, (Jeffamine® DU-700, obtained from Huntsman, which also contains a urea linkage in the middle), isophorone diisocyanate (IPDI, obtained from Bayer), and 1,3 diamino pentane (DYTEK® EP, obtained from Dupont). Silicone polyureas containing 20, 35, 45 and 65 wt% hard segment (defined as the combined wt% of IPDI and DYTEK® EP chain extender) were prepared by adding a stoichiometric amount of IPDI, dropwise, to a solution of the three diamines in isopropyl alcohol, while stirring. The reactions were carried out at a 15% concentration in the isopropyl alcohol at room temperature in a 1-liter round bottom flask purged with dry nitrogen, with a batch size of 0.5 liters. The completion of the reactions, typically within 4 hours of stirring, was confirmed by amine titration and FTIR analysis. The silicone polyurea samples will be referred to, for example, as 25/55/20, indicating 25 wt% polydimethylsiloxane (PDMS), 55 wt% Jeffamine® DU-700, and 20 wt% hard segment. The molar ratios of the components used for the four different silicone polyureas are given in Table I.

Bulk Characterization of Silicone Polyureas

Films roughly 0.3 mm thick for transmission electron microscopy (TEM), differential scanning calorimetry (DSC), and dynamic

TABLE I Molar ratios of components used for silicone polyureas

Silicone polyurea	*Silicone diamine moles*	*Jeffamine® DU700 moles*	*DYTEK® EP moles*	*IPDI moles*
25/55/20	1.0	12.2	3.3	16.5
25/40/35	1.0	8.9	14.8	24.7
25/30/45	1.0	6.7	22.5	30.2
25/10/65	1.0	2.2	37.9	41.1

mechanical thermal analysis (DMTA) were prepared by casting from 15 wt% solutions in isopropyl alcohol into glass Petri dishes. Drying was carried out at room temperature, followed by placing the films in a vacuum oven at 65°C for several hours to assure complete removal of the isopropyl alcohol. Thin sections for TEM were prepared by cryoultramicrotomy at −125°C using a dry-knife technique. The sections (unstained) were examined at 100 kV in the bright field mode of a JEOL 100CX transmission electron microscope. The polydimethylsiloxane (PDMS) domains appear dark upon exposure to the electron beam. DSC was carried out using a Perkin-Elmer DSC-4 at a heating rate of 20°C/min. DMTA was accomplished using a Rheometrics Solid Analyzer (RSA-2) in the rectangular tension mode at a frequency of 1 Hz and a heating rate of 2°C/min.

Surface and Interfacial Characterization of Silicone Polyureas

Coatings used for surface and interfacial analyses were prepared by coating a 2.5 wt% solution in isopropyl alcohol onto a PET film substrate using a #6 coating rod, followed by drying for 10 minutes at 65°C (giving a silicone polyurea film thickness of about 0.15 micron).

Contact angle measurements were made using the sessile drop method with a Rame Hart goniometer equipped with an environmental chamber. Water and methylene iodide used for contact angle measurements were distilled, while the hexadecane was used as received. Advancing and receding contact angles were obtained by increasing or decreasing the drop volume until the three-phase boundary moved over the coating surface. The capillary pipette of the microsyringe was kept immersed in the drop during the entire measurement. The contact angles reported here are the averages of measurements made on 4 to 6 different drops.

X-ray photoelectron spectroscopy (XPS) and static secondary ion mass spectrometry (SIMS) were done using a Perkin–Elmer Physical Electronics 5100XPS/6000SSIMS instrument. For XPS, Mg $K\alpha_{12}$ incident X-rays and a hemispherical analyzer were used. The angle, θ, between the sample surface and the analyzer (takeoff angle) was varied between 15 and 90 degrees. The depth in the sample, normal to the surface, from which 95% of the observed signal intensity is derived is

given roughly as $3\lambda \sin\theta$, where λ is the inelastic mean free path of the photoelectrons [39]. For organic materials, and the experimental conditions used here, λ will be roughly 30 Å [40]. Therefore, sampling depths for takeoff angles of 15, 30, 55 and 90 degrees are about 25, 45, 75 and 90 Å, respectively. Atomic concentrations were determined by normalizing the areas under the high-resolution spectra of each element by the atomic sensitivity factors determined for the instrument (using a series of homopolymers of known composition).

For static SIMS, a differentially pumped ion gun, a low energy electron flood gun (model 04-085), and a quadrupole mass spectrometer (m/z 0-800) were used. The analyzer was positioned to collect ions normal to the sample surface, while the ion beam was oriented at a glancing angle to the surface. The incident ions were a defocussed beam of 3.5 keV Xe^+ ions, with a beam current density of 1.5 nA/cm^2. All data was collected on samples exposed to $< 10^{13}$ ions/cm^2 total ion dose in order to remain within the static regime. Both positive and negative ion spectra were obtained. The sampling depth with static SIMS has been reported to be on the order of 10 Å [39].

The same coatings used for surface analysis were also used for adhesion measurements. A polypropylene-backed tape having a 1-mil-thick coating of an alkyl acrylate based pressure sensitive adhesive (PSA), containing 5 wt% acrylic acid comonomer, was used as a test tape. One-inch-wide strips of tape were rolled down onto the silicone polyurea coatings using 6 passes from a 2 Kg roller. Aging was done for various lengths of time (30 seconds to 4 weeks) and at various temperatures (between 21°C and 65°C) prior to peel testing, which was all done at 21°C and 50% relative humidity. A separate sample was used for each aging condition. For heat aging experiments, the PSA tape/silicone polyurea release coating composite samples were placed between preheated glass plates in the oven. After heat aging, the samples were removed from the oven and allowed to cool for 15 minutes prior to peel testing. The 180° peel force was measured at a peeling rate of 90 inches/min using an Instrumentors Inc. slip peel tester. The reported peel force is the average over a 5-second time interval.

Samples for studying the effect of water immersion were prepared by dipping the silicone polyurea coated PET films into a water bath for 2 minutes, at the desired temperature, followed by quenching of the

films in an ice water bath. A separate film was used for each immersion temperature studied.

RESULTS AND DISCUSSION

Bulk Characterization of Silicone Polyureas

Figure 1 shows a TEM micrograph of the 25/35/45 silicone polyurea sample. The PDMS phases appear dark in the micrograph. Discrete spherical PDMS domains, approximately 200 Å in diameter, are observed. Similar morphologies were observed for all the other silicone polyureas studied here. The TEM results confirm that the PDMS segments of the silicone polyureas are well phase separated from the hard segments and polypropylene oxide segments. In order to establish the degree of phase separation between the hard segments and polypropylene oxide segments, both DSC and DMTA were employed.

Figure 2 shows DSC traces of the silicone polyureas at temperatures from $-75°C$ to over 200°C. The Jeffamine® DU700 polypropylene

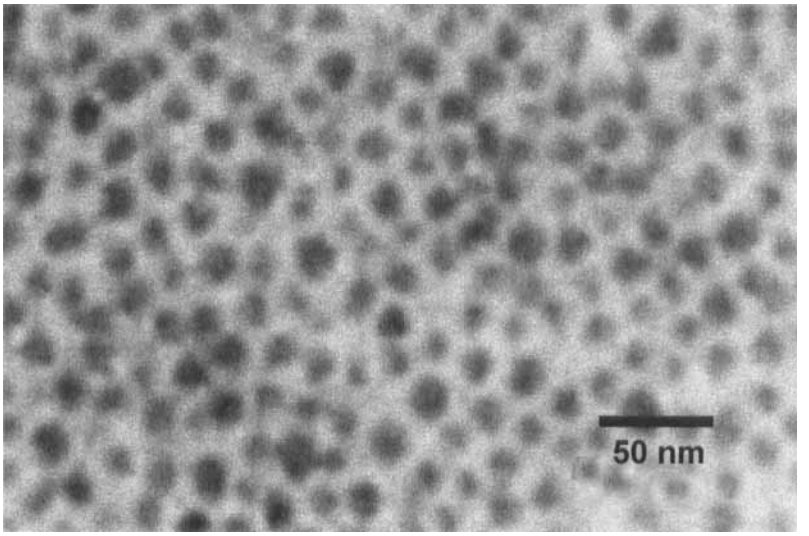

FIGURE 1 Transmission electron micrograph of the 25/35/45 silicone polyurea. The siloxane phases appear dark in the micrograph.

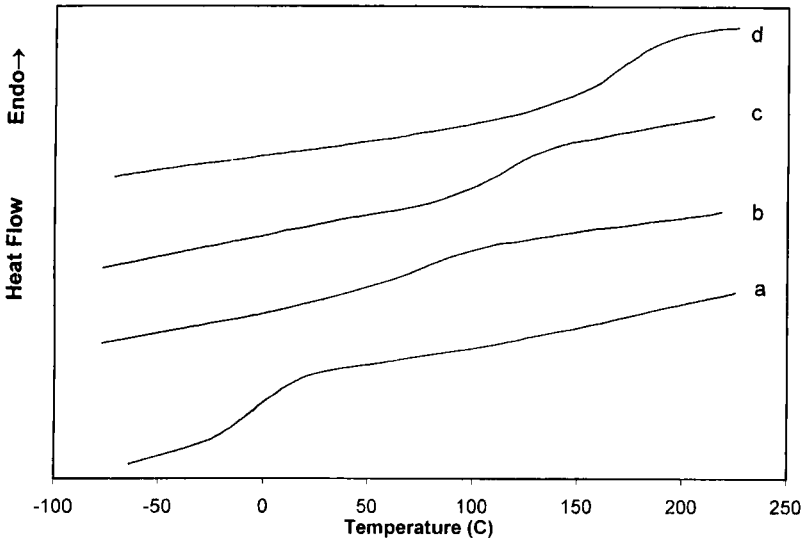

FIGURE 2 Differential Scanning Calorimetry traces of silicone polyureas containing: (a) 20 wt% hard segment, (b) 35 wt% hard segment, (c) 45 wt% hard segment, and (d) 65 wt% hard segment.

oxide diamine exhibits a T_g of $-60°C$ when tested by DSC, which is close to the literature value of $-75°C$ for polypropylene oxide [41]. There is no evidence of a glass transition due to a polypropylene-oxide-rich phase for the silicone polyureas studied here. A single glass transition is observed between $-75°C$ and 200°C, with the (midpoint) T_g increasing steadily from $-1°C$ at 20 wt% hard segment to 170°C at 65 wt% hard segment. Figure 3 gives the tensile storage modulus (E') and tan delta *vs.* temperature data for the silicone polyureas, at temperatures between $-100°C$ and 200°C. Over this temperature range, a single rheological transition is observed, with the temperature of the transition increasing with increasing hard segment content in the silicone polyurea. (Although not shown here, a slight transition was observed at about $-125°C$ for all the samples, attributed to the T_g of the phase-separated PDMS domains.) Again, there is no evidence of a polypropylene-oxide-rich phase in these silicone polyureas. The transitions observed by DSC and DMTA can be attributed to the glass transition of a non-silicone matrix phase consisting of a mixture of the hard segments and the short polypropylene oxide segments.

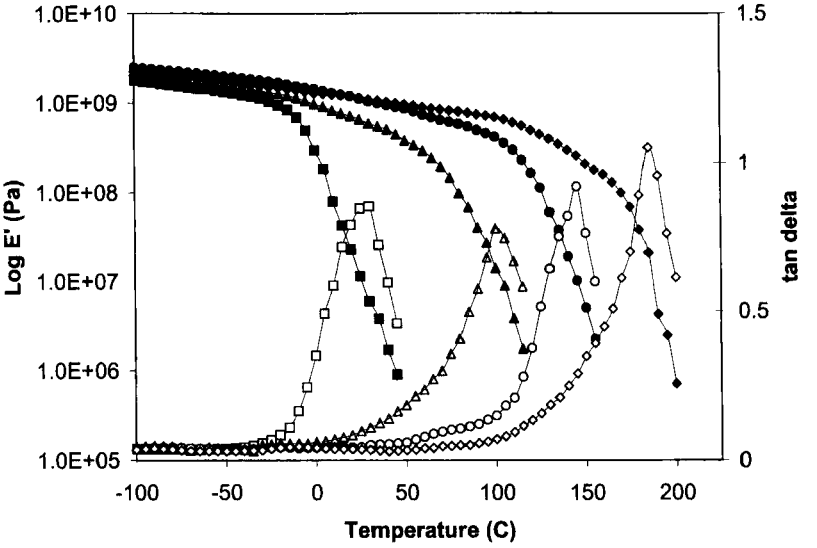

FIGURE 3 Log E' (filled data points) and tan delta (open data points) *vs.* Temperature plots for silicone polyureas containing 20 wt% hard segment (squares), 35 wt% hard segment (triangles), 45 wt% hard segment (circles), and 65 wt% hard segment (diamonds).

TABLE II Transition temperatures of silicone polyureas

Silicone polyurea	*DSC* T_g (°C)	(*Tan delta*)$_{max}$ *temp* (°C)
25/55/20	−1	27
25/40/35	74	101
25/30/45	116	145
25/10/65	170	187

The glass transition temperature increases systematically as the weight ratio of hard segments to polypropylene oxide segments increases. Table II lists the T_gs and (tan delta)$_{max}$ temperatures determined by DSC and DMTA measurements, respectively. The temperatures of the tan delta maxima are roughly 20 to 30 degrees higher than the corresponding T_gs determined by DSC, as is often observed. Although not discussed in this paper, it has been seen that silicone polyureas made with higher polypropylene oxide segment molecular weights do exhibit a phase-separated, polypropylene-oxide-rich phase, *i.e.*, a three-phase microdomain structure.

Surface Characterization of Silicone Polyureas

Table III lists the advancing contact angles of water and hexadecane for the silicone polyurea coatings. The contact angles were measured roughly 10 seconds after the advancement of the liquid drops. In addition, the dispersive and polar contributions to the surface energies of the coatings were calculated from the dispersive and polar surface tension components of water and hexadecane, using the geometric mean equation [42]. Similar results are obtained for all coatings, with the calculated surface energies being almost entirely dispersive, between 21 and 22 mJ/m^2. The surface energies of polydimethylsiloxane and poly(propylene oxide) are reported [42] to be 20 mJ/m^2 and 31 mJ/m^2, respectively, and the surface energies of the polar urea segments are expected to be even higher. Therefore, the contact angle results indicate a high concentration of the polydimethylsiloxane segments at the coating surface.

The surface composition of the silicone polyurea coatings was examined further using X-ray photoelectron spectroscopy (XPS). For example, Figure 4 shows the C1s spectra for the 25/40/35 silicone polyurea coating, at takeoff angles of 15 and 90 degrees. The main peak in the C1s spectra, centered at a binding energy of about 284.6 eV, can be assigned to C—C or C—Si type bonding. At the larger sampling depth, a shoulder appears on the main peak at a slightly higher binding energy (1.5 to 2 eV higher) due to carbons singly-bonded to either oxygen or nitrogen. There is also a peak that develops at about 289 eV due to the carbons doubly-bonded to oxygen (carbonyl carbons) in the urea groups. Similar C1s spectra *versus* takeoff angle were observed for the other silicone polyurea coatings, consistent with an enrichment of polydimethylsiloxane, and a depletion of the polypropylene oxide soft segments and urea hard segments at the surface of the coatings. Table IV lists the atomic

TABLE III Advancing contact angle analysis of silicone polyurea coatings

Silicone polyurea	θH_2O ($\pm 2°$)	$\theta C_{16}H_{34}$ ($\pm 2°$)	γ^d (mJ/m^2) (± 0.5)	γ^p (mJ/m^2) (± 0.1)
25/55/20	110	37	22.1	0.1
25/40/35	109	38	21.8	0.2
25/30/45	109	39	21.6	0.2
25/10/65	110	38	21.8	0.1

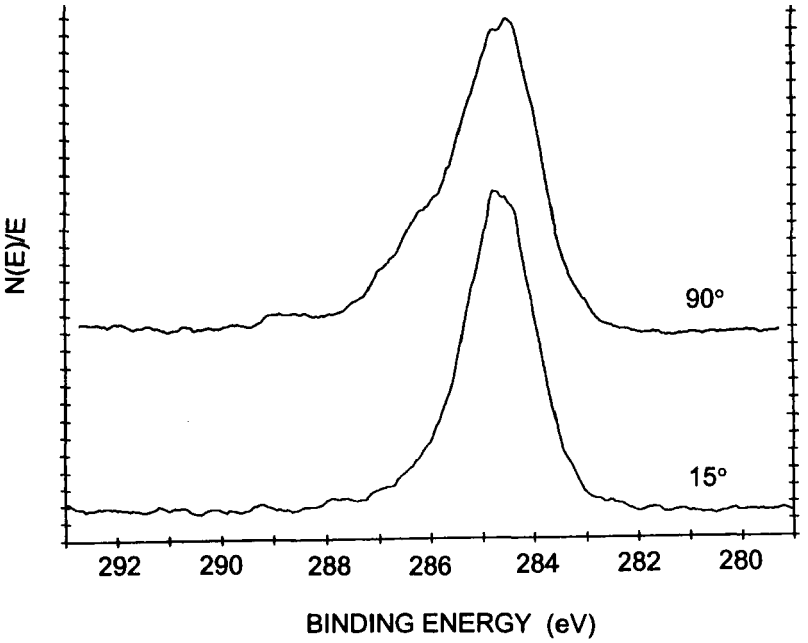

FIGURE 4 XPS C1s spectra of the 25/40/35 silicone polyurea at takeoff angles of 15 and 90 degrees.

concentrations determined at the various takeoff angles, in addition to the bulk atomic concentrations calculated from the overall chemical composition of the silicone polyureas (neglecting the H atoms). As the sampling depth (takeoff angle) is decreased, the compositions approach that of polydimethylsiloxane (50% C, 25% O, 25% Si), indicating a high concentration of polydimethylsiloxane segments at the coating surface, and a depletion of the urea hard segments and polypropylene oxide soft segments. At larger depths, the compositions approach the average (bulk) compositions of the silicone polyureas.

The angle-resolved atomic concentration data were inverted, following the method outlined by Tyler *et al.* [43], to obtain atomic concentration *versus* depth data. The photoelectron mean free paths used in the data inversion were obtained from the equation $\lambda = 0.087E^{1/2}$, as suggested by Seah and Dench [40], where E is the photoelectron energy. Figure 5 shows the atomic concentration *versus* depth profiles calculated for the 25/10/65 silicone polyurea coating. It is evident that roughly the top 15 to 20 Å of the coating consists

TABLE IV XPS atomic conc. *vs.* takeoff angle for silicone polyurea coatings

Silicone polyurea	*Takeoff angle*	*%C*	*%O*	*%Si*	*%N*
25/55/20	15	55.9	23.3	20.5	0.3
	30	56.8	22.6	19.7	0.9
	55	58.5	22.4	17.1	2.0
	90	60.6	22.0	14.8	2.7
	Bulk	66.7	21.4	5.0	6.9
25/40/35	15	55.3	23.4	20.9	0.5
	30	56.4	22.4	19.6	1.5
	55	58.5	22.4	16.5	2.6
	90	59.5	21.8	15.0	3.7
	Bulk	67.4	18.8	5.0	8.8
25/30/45	15	53.9	24.1	21.5	0.5
	30	55.4	23.0	19.9	1.8
	55	58.2	21.7	16.6	3.5
	90	59.5	21.4	14.7	4.4
	Bulk	67.8	17.1	5.0	10.1
25/10/65	15	52.9	24.0	22.5	0.6
	30	54.0	23.0	21.2	1.8
	55	56.8	21.8	17.7	3.8
	90	58.8	20.6	15.9	4.7
	Bulk	68.7	13.6	5.0	12.7
25/10/65 Aged 3 days at 65°C against PSA	15	57.4	23.2	17.6	1.9
	30	60.4	21.8	14.7	3.1
	55	63.5	20.0	11.6	4.9
	90	64.6	19.2	10.3	5.9

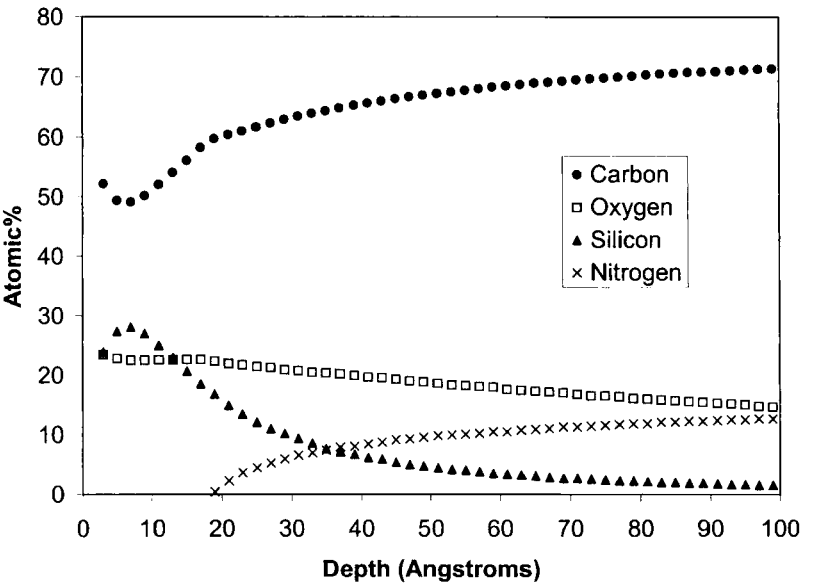

FIGURE 5 Atomic concentration *vs.* depth profiles for the 25/10/65 silicone polyurea, obtained by inverting the angle-resolved XPS data.

predominantly of polydimethylsiloxane, and that the polydimethylsiloxane (silicon) concentration falls off quickly at larger depths. In addition, the top 20 Å of the coating is devoid of urea linkages (nitrogen). Similar results were seen for the other silicone polyurea coatings.

The surface composition of the silicone polyurea coatings was also examined by static SIMS. Both the positive and negative ion spectra of the silicone polyurea coatings were indistinguishable from the spectra of pure polydimethylsiloxane, providing further evidence of a polydimethylsiloxane overlayer (at least about 10 Å thick) at the coating surface.

The picture which emerges for the morphology of the silicone polyureas is shown schematically in Figure 6a. In the bulk, the silicone

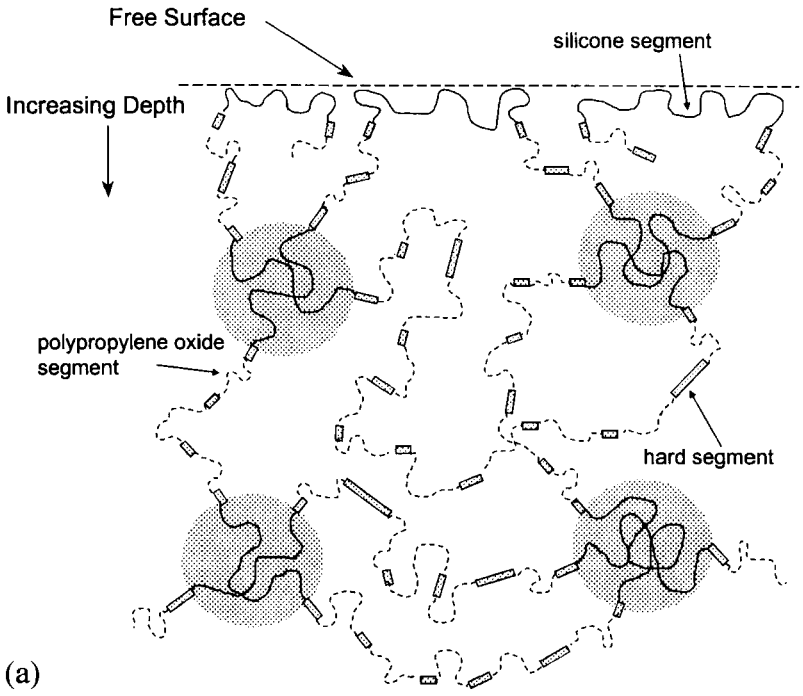

FIGURE 6 Schematics of the bulk, surface, and interfacial structure of the silicone polyureas. The silicone segments form discrete spherical domains in the bulk and accumulate at the coating surface, as shown in 6a. Upon contact with an orienting medium, a restructuring may occur, whereby the silicone segments migrate away from the interface, as shown in 6b.

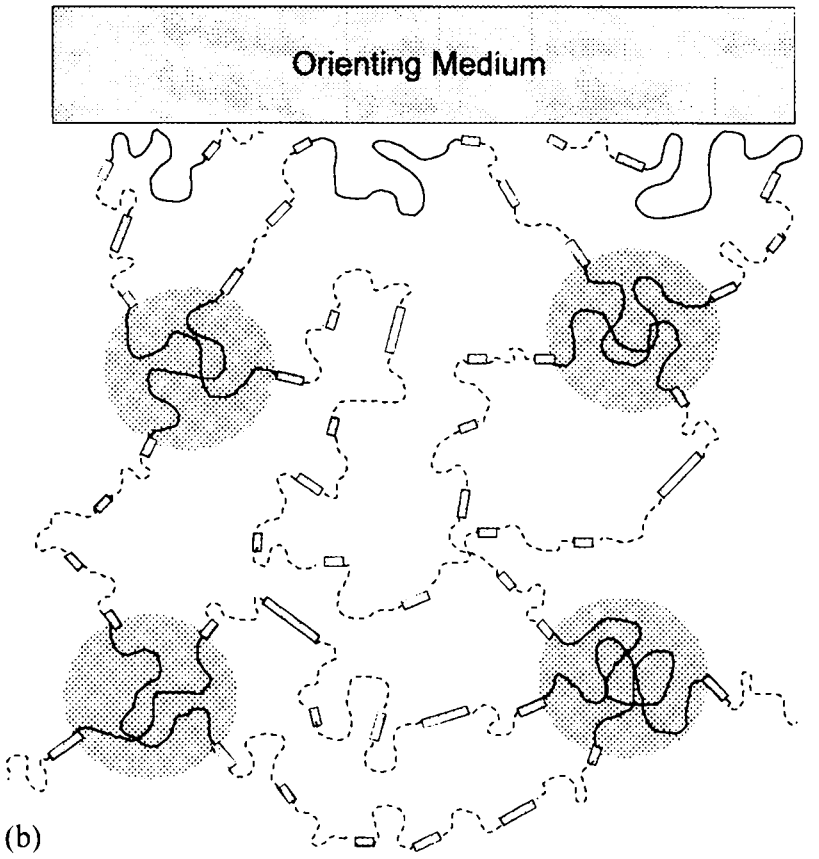

FIGURE 6 (Continued).

segments form spherical microdomains, with the hard segments and polypropylene oxide soft segments forming a mixed matrix region. The surface of the silicone polyureas is covered by a thin overlayer, roughly 15 to 20 Å thick, of the polydimethylsiloxane segments. The unperturbed root mean square end to end distance for 5,000 molecular weight polydimethylsiloxane segments is roughly 50 Å [41]. The thickness of the polydimethylsiloxane surface layer is considerably less than this value, which indicates that the polydimethylsiloxane segments at the surface are stretched in the plane of the film. Since the siloxane segments are connected to the other polymeric segments, chain packing requirements limit the amount of silicone that can be

present at the surface. However, since the siloxane segments are highly flexible, they can stretch from their unperturbed conformation in order to cover the surface of the coating and minimize the surface energy.

Interfacial Characterization of Silicone Polyureas

It is well known that polymer surfaces can undergo segmental restructuring or rearrangements upon contact with another medium, in order to minimize the interfacial energy. Therefore, studies were conducted to examine the response of the silicone polyurea surfaces, upon contact with different orienting media, as a function of the silicone polyurea composition. If the orienting medium has a favorable specific chemical interaction with a non-silicone portion of the silicone polyurea, and the segmental mobility in the near surface region of the silicone polyurea coating is high enough, an interfacial restructuring may occur, as shown schematically in Figure 6b, whereby the non-silicone segments come into contact with the orienting medium. For example, upon contact with water, it is expected that there would be a driving force for the hydrophobic polydimethylsiloxane segments to migrate away from, and for the more polar hard segments (urea groups) to migrate towards, the interface with water. Measurements of the receding water contact angle, as a function of the water dwell time (amount of time that the water droplet was allowed to contact the surface prior to receding the water droplet), were made at room temperature for the four different silicone polyurea formulations. The results are shown graphically in Figure 7, which shows the cosine of the receding water contact angle for water dwell times up to 5 minutes. Also included are the results for a crosslinked polydimethylsiloxane coating as a reference. For comparison, polyureas having compositions similar to the silicone polyureas studied here, except that no silicone segments were incorporated, were also examined. The receding water contact angle of the crosslinked polydimethylsiloxane reference is high, and remains high with increasing water dwell time. In contrast, the receding water contact angles of the silicone polyurea coatings are all reduced relative to the polydimethylsiloxane standard, even when measured with as little water dwell time as possible (initial receding contact angle). The initial receding contact angle is seen to decrease as the amount of hard segment in the polyurea is decreased. In fact, at 20 wt% hard segment, the receding water contact angle is similar to that

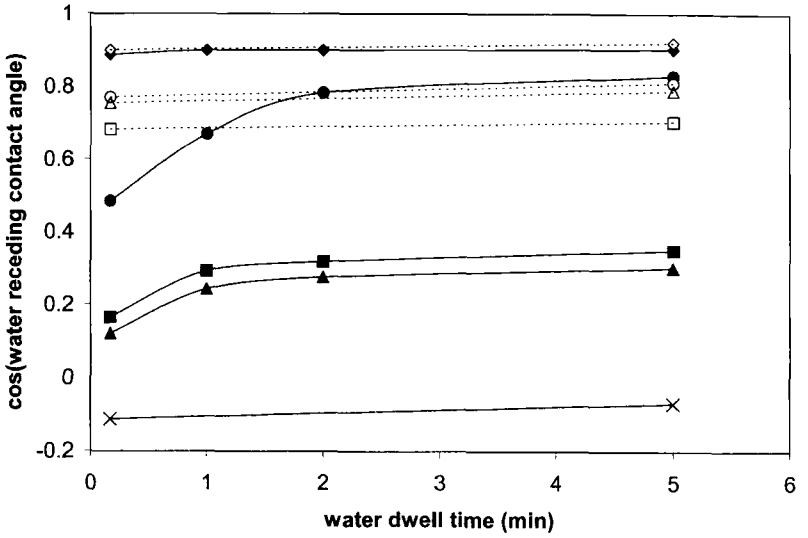

FIGURE 7 Cosine of the water receding contact angle *versus* the water dwell time, at room temperature, for the silicone polyureas containing 65 wt% hard segment (filled triangles), 45 wt% hard segment (filled squares), 35 wt% hard segment (filled circles), and 20 wt% hard segment (filled diamonds). Also shown are the corresponding data for the polyureas without silicone segments: 0/10/65 (open triangles), 0/30/45 (open squares), 0/40/35 (open circles), and 0/55/20 (open diamonds), as well as for a crosslinked polydimethylsiloxane network (X).

of a comparable polyurea having no silicone segments, at all water dwell times. For the other silicone polyureas the receding contact angle decreases with increasing dwell time of the water. It appears that most of the change in contact angle occurs within the first 2 minutes. For the silicone polyureas with 45 wt% or 65 wt% hard segment, the contact angle practically stabilizes at an intermediate value between that of pure polydimethylsiloxane and that of the corresponding polyurea containing no silicone. At 35 wt% hard segment, the receding contact angle after 5 minutes dwell time approaches that of the corresponding polyurea containing no silicone. These results indicate that significant changes in the surface composition of the silicone polyurea coatings can occur upon contact with water, even at temperatures significantly lower than the glass transition temperature of the non-silicone matrix. Recall that the T_g of the 25/10/65 silicone polyurea is about 150°C higher than room temperature, yet the receding water contact angle is decreased markedly from that of a polydimethylsiloxane coating after only a few minutes contact. For the silicone polyurea containing 20

wt% hard segment, which has a matrix T_g about 20°C below room temperature, it appears that the silicone migrates away from the interface with water in less than the time it takes to make an initial contact angle measurement (*i.e.*, about 5 seconds or less). For silicone polyureas having higher non-silicone matrix T_gs, significant levels of silicone can be maintained at the interface for longer periods of time. This enhanced surface mobility relative to that in the bulk has been previously noted by Kajiyama *et al.* [44], who studied polystyrene–polymethylmethacrylate diblock copolymers and found extensive surface restructuring at temperatures 50°C less than the polystyrene block T_g. The rates of restructuring observed for the silicone polyureas studied here are relatively high compared with those reported for other silicone-containing polyurethanes [5, 6] or polyurethane-ureas [37]. This difference is due, at least in part, to the mixing of the short polypropylene oxide segments into the hard segments of our silicone polyureas. This mixing reduces the hard segment T_g and increases the segmental mobility within the polymer.

The effect of temperature on the water receding contact angles has also been studied. For example, Figure 8 shows the water receding contact angle *versus* water dwell time for the 25/30/45 silicone polyurea coating, at temperatures of 21°C, 50°C and 65°C. In addition, the receding contact angle data for the corresponding polyurea that does not contain silicone (0/30/45) are also shown at the three temperatures. The receding contact angles of the 0/30/45 polyurea are quite low and change little with increasing water dwell time or increasing temperature. In contrast, the receding water contact angle of the 25/30/45 silicone polyurea decreases more rapidly as the temperature is increased, indicating a more rapid rate of restructuring of the silicone polyurea at the interface with water. At 50°C, the receding water contact angle of the 25/30/45 silicone polyurea approaches that of the polyurea containing no silicone after a water dwell time of about 10 minutes, while at 65°C this transition takes only 2 minutes. In contrast, the receding water contact angle decreases much more slowly at room temperature.

An alkyl-acrylate-based pressure sensitive adhesive (PSA) containing 5 wt% acrylic acid was also investigated as an orienting medium. The force required to peel a polypropylene-backed tape coated with this acrylate PSA from the silicone polyurea coatings was measured

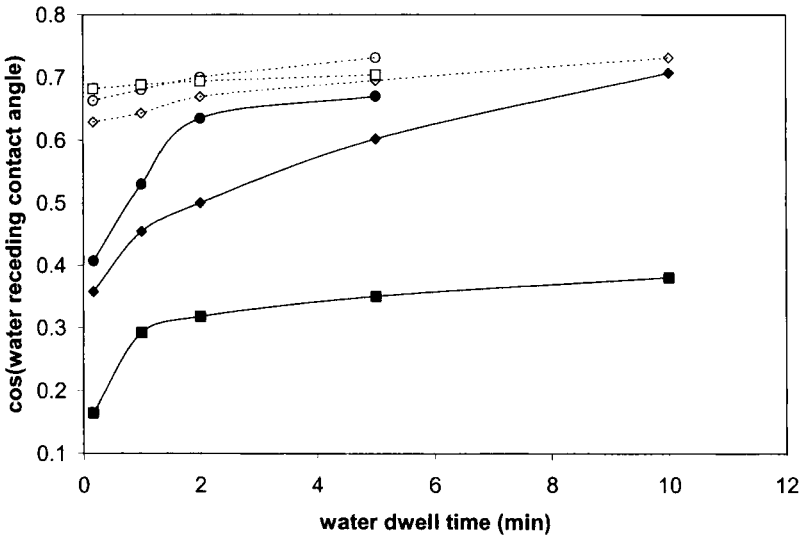

FIGURE 8 Cosine of the receding water contact angle *versus* the water dwell time for the 25/30/45 silicone polyurea at 21°C (filled squares), 50°C (filled diamonds), and 65°C (filled circles). Also shown are the corresponding data for the 0/30/45 polyurea that does not contain silicone at 21°C (open squares), 50°C (open diamonds), and 65°C (open circles).

as a function of aging time and temperature. Figure 9 shows the measured peel forces *versus* room temperature aging time for the various silicone polyureas. Room temperature aging times between 30 seconds (initial) and 1 month were studied. Note that, except for the silicone polyurea containing 20 wt% hard segment, the initial peel forces of the PSA tape are quite low at about 1 oz/in (30 g/inch, 12 g/cm), typical of a silicone liner. Recall that initially, prior to PSA contact, all of the silicone polyurea coatings exhibited a thin overlayer of silicone at their surface, which can account for the low initial peel forces. However, the peel forces increase significantly with increasing aging time, especially for the silicone polyureas with lower hard segment contents. It should be noted that at peel forces below about 60 oz/in (670 g/cm), XPS and static SIMS measurements of the silicone polyurea and acrylate PSA surfaces, after peeling them apart, reveal that the failure mode is predominantly adhesive, *i.e.*, at the polyurea/PSA interface. However, at peel forces greater than about 60 oz/in (670 g/cm), the locus of failure was actually within the PSA layer. At

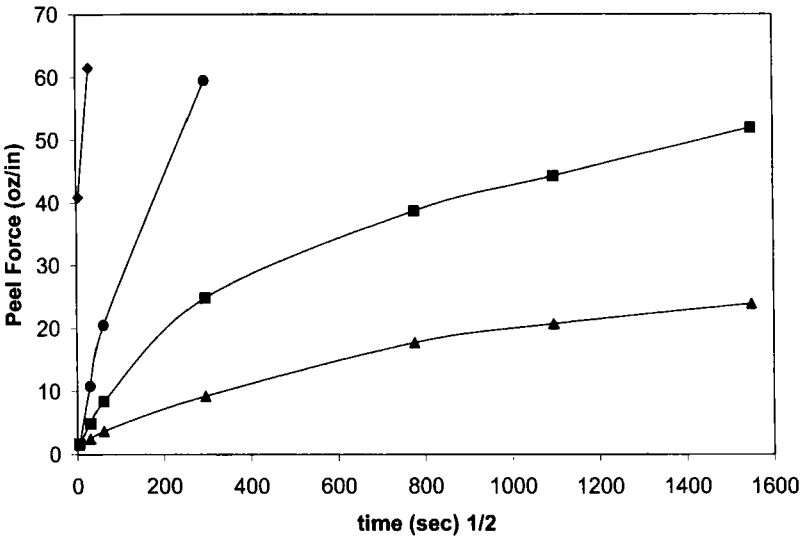

FIGURE 9 Peel Force of the acidic acrylate PSA based tape *versus* (aging time)$^{1/2}$, at room temperature, for the silicone polyureas containing 20 wt% hard segment (diamonds), 35 wt% hard segment (circles), 45 wt% hard segment (squares), and 65 wt% hard segment (triangles).

20 wt% hard segment, the peel force increases to the point that a cohesive split of the PSA is seen after only 15 minutes aging time. This "build" in adhesion is slowed down somewhat at 35 wt% hard segment, where one-day aging is required before the cohesive split of the PSA is observed. At 45 wt% and 65 wt% hard segment, the peel forces increase even more slowly, such that adhesive failures are observed after one month of room temperature aging. However, even at 65 wt% hard segment the peel force has increased by over a factor of 20 from the initial value after one month aging.

Figure 10 shows the peel force *vs.* aging time for the 25/30/45 and 25/10/65 silicone polyurea coatings for aging temperatures of 20°C, 50°C and 65°C. Increasing the aging temperature results in an increase in the rate of adhesion build. For the 25/30/45 silicone polyurea, the adhesion builds to the point that a cohesive split of the PSA is observed after 1 day at 50°C and after only 15 minutes at 65°C. In the case of 65 wt% hard segment, the rate of adhesion build is much slower, and the PSA can still be cleanly removed from the silicone polyurea coating after long term aging at 65°C. Note that the peel

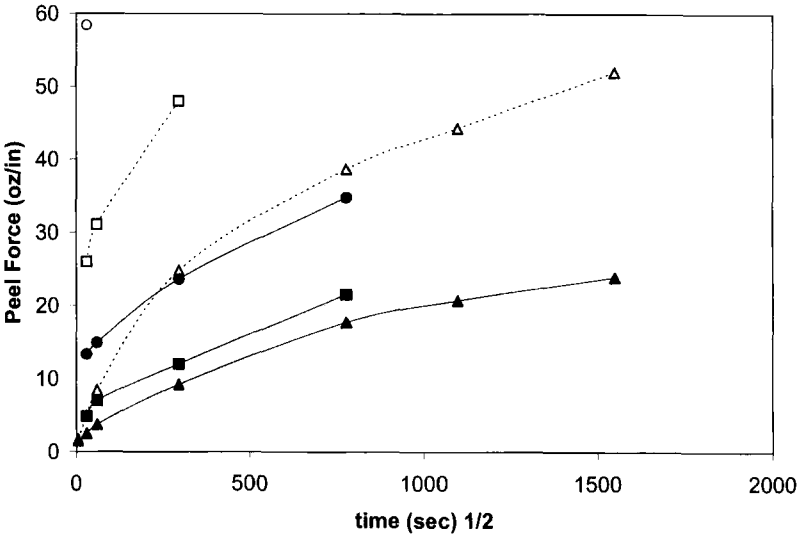

FIGURE 10 Peel Force of the acidic acrylate PSA based tape *versus* (aging time)$^{1/2}$, for the 25/30/45 silicone polyurea after aging at 21°C (open triangles), 50°C (open squares), and 65°C (open circle) and for the 25/10/65 silicone polyurea after aging at 21°C (filled triangles), 50°C (filled squares), and 65°C (filled circles).

force *vs* time response for the 25/10/65 silicone polyurea aged at 65°C is roughly similar to that of the 25/30/45 silicone polyurea aged at room temperature, and the peel force *vs.* time response for the 25/30/45 silicone polyurea aged at 50°C is roughly similar to that of the 25/40/35 silicone polyurea aged at room temperature.

The build in peel force can be attributed to an interfacial restructuring at the silicone polyurea/PSA interface, whereby the non-silicone segments in the silicone polyurea (*e.g.*, the urea groups) migrate towards the interface with the PSA, and the silicone segments in the silicone polyurea migrate away from the interface, as shown schematically in Figure 6b. In the case of an acrylate PSA containing acrylic acid, there is the potential for acid-base interactions between the acrylic acid in the PSA and the basic urea groups in the polyurea, and these specific favorable chemical interactions provide the driving force for the interfacial restructuring. The rate of increase in peel force with increasing aging time and/or temperature is expected to be dependent on the degree of segmental mobility in the polyurea coating near the interface with the PSA. Polyureas containing lower levels of

hard segment (*e.g.*, 20 wt%) have a high degree of segmental mobility and, therefore, exhibit high peel forces even at short dwell times. Polyureas containing higher amounts of hard segment, and, thus, higher T_gs, have reduced mobility in the non-silicone matrix phase and, therefore, exhibit reduced rates of build in the peel force. Note that, even when the aging temperature is well below the non-silicone matrix T_g, significant restructuring at the interface can still occur, as evidenced by the increased adhesion. For example, the matrix T_g of the 25/10/65 silicone polyurea is about 150°C higher than room temperature, yet a significant build in peel force is still observed at room temperature. This result indicates that the segmental mobility within the silicone polyurea is higher at the surface (or interface) than it is in the bulk, consistent with the water receding contact angle measurements described earlier.

The absolute magnitude of the peel force between the PSA and the silicone polyurea coatings is determined by the rheology of the PSA and the silicone polyurea coatings as well as the chemical interactions at their interface. It is expected that the rheology of the PSA will have a greater impact than the rheology of the silicone polyurea coating, considering that the silicone polyurea coating is quite thin. For the present studies the PSA is kept constant, and only the silicone polyurea formulation is changed. As shown in Figure 3, at the temperature where the peel measurements are made (21°C), the silicone polyureas containing 35 wt%, 45 wt%, and 65 wt% hard segment have similar storage modulii and tan delta values since they all have glass transition temperatures significantly greater than room temperature. Since the viscous flow component of these three materials is low, the rheology of these coatings is not expected to play a significant role in determining their peel forces. The only silicone polyurea which has significantly different modulus and tan delta values at room temperature is the one containing 20 wt% hard segment, for which the tan delta is maximized near room temperature. The high initial peel forces for this silicone polyurea may be caused in part by the ability of this coating to dissipate energy during peel, in addition to the rapid interfacial restructuring, as discussed previously, that results in greater interfacial adhesion.

XPS was used to examine the changes in surface composition of the silicone polyureas upon aging against the acrylate PSA. For example,

Table IV lists the atomic concentrations *vs.* takeoff angle for a 25/10/65 silicone polyurea coating after aging against the acrylate PSA for 3 days at 65°C (the peel force of the PSA tape was 30 oz/in (335 g/cm) after this aging). Note the increase in the concentration of nitrogen and carbon and the decrease in the concentration of silicon near the surface after aging against the PSA. At a 15-degree takeoff angle (smallest sampling depth) the concentration of nitrogen has increased by over a factor of three, indicating a large increase in the concentration of urea groups at the interface with the PSA. The silicon concentration in this region drops by about 25%, indicating that the silicone segments have migrated away from the PSA interface to a significant extent.

Further investigations of the response of silicone polyurea surfaces upon contact with water were carried out, by immersing the coatings in water at various temperatures followed by surface analysis and adhesion measurements to probe the changes in surface composition. After the coatings were immersed in the heated water for 2 minutes they were quenched by adding ice water to the bath in order to try to lock in the surface structure. However, once the films are removed from the water bath and exposed again as a free surface, some degree of surface restructuring is expected to occur since the silicone segments will want to migrate back towards the free surface. For this reason, depending on the segmental mobility of the particular silicone polyurea studied, and the amount of time between removing the film from the water and carrying out the surface analysis, this type of experiment may not capture all of the restructuring due to the exposure to water. For example, for the 25/55/20 silicone polyurea coating that had been immersed in water at 80°C, the advancing and receding water contact angles were very close to those measured on the coating prior to water immersion. In this case, the restructuring that had taken place in the water bath was quickly recovered once the coating was exposed again as a free surface, due to the high degree of segmental mobility for this silicone polyurea formulation at room temperature. For silicone polyureas with higher hard segment contents, and lower segmental mobility, part of the restructuring occurring in the water bath at elevated temperatures can be captured by the quenching procedure used here. For example, Figure 11 shows the cosine of the receding contact angles of water and methylene iodide *versus* water immersion temperature (up to 80°C) for the 25/30/45

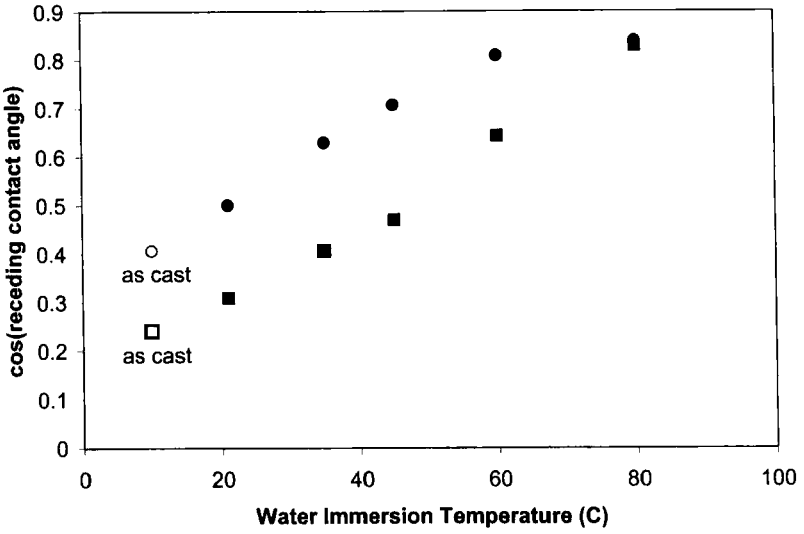

FIGURE 11 Cosine of the receding water (filled squares) and methylene iodide (filled circles) contact angles *versus* water immersion temperature for the 25/30/45 silicone polyurea following a 2-minute water immersion. The receding contact angles for the as-cast film are also shown (unfilled data points).

silicone polyurea. The contact angles were measured within 10 minutes of removing the coatings from the water bath. The receding contact angles of water and methylene iodide decrease markedly as the water immersion temperature increases, indicating that a significant restructuring takes place fairly quickly upon contact with water, especially at the higher temperatures. In contrast to the case of the silicone polyurea containing only 20% hard segment, a significant amount of the restructuring that had taken place against the water could be captured for the silicone polyurea containing 45% hard segment. It should be noted that, upon annealing (10 minutes at 100°C) of the 25/30/45 film that had been immersed in water at 80°C, the original water contact angles were nearly recovered, indicating the reversible nature of the restructuring under the right conditions.

XPS was also used to analyze the changes in silicone polyurea surface composition upon exposure to water. For example, Figure 12 shows the atomic% nitrogen and % silicon *vs.* sin(takeoff angle) for the 25/30/45 silicone polyurea coating, as prepared, and after immersion in water at temperatures up to 80°C. The XPS measurements were done within 30 minutes after removing the films from the

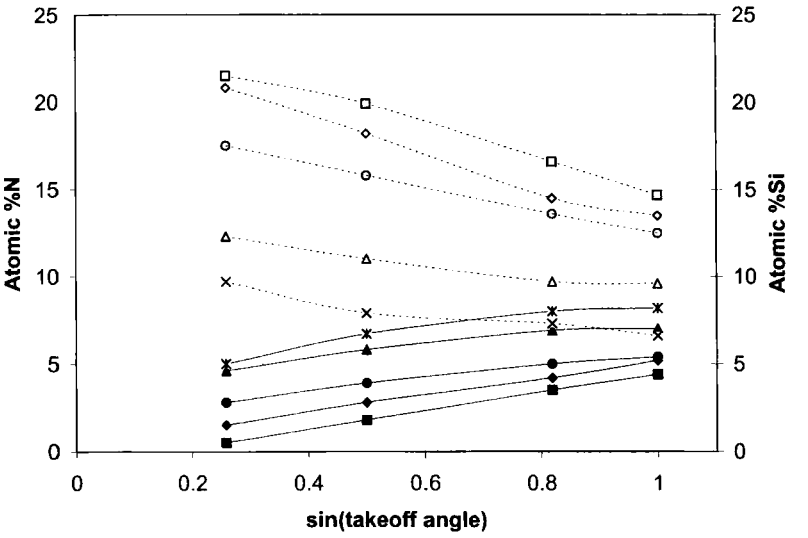

FIGURE 12 XPS atomic percent nitrogen (filled data points) and silicon (open data points) *versus* sin(takeoff angle) for the 25/30/45 silicone polyurea as-cast (squares) and after water immersion for 2 minutes at 21°C (diamonds), 45°C (circles), 60°C (triangles), and 80°C (X).

water bath. As the water immersion temperature is increased, the nitrogen content at the silicone polyurea surface increases and the silicon concentration decreases. For example, at a 15-degree takeoff angle, the nitrogen concentration increases from the initial value of 0.5 atomic% to 5 atomic%, and the silicon concentration decreases from an initial value of 21.5 atomic% to 9.7 atomic% after the 2-minute water immersion at 80°C. The atomic concentrations at the 90-degree takeoff angle after the 80°C immersion are 8.2% nitrogen and 6.6% silicon, close to the calculated bulk compositions of 10.1% nitrogen and 5.0% silicon. These results are consistent with a restructuring of the silicone polyurea near the interface with the water, whereby the silicone segments migrate away from, and the urea groups migrate towards, the interface with water. The rate and extent of restructuring increases with increasing water temperature.

The peel force of the alkyl-acrylate-based PSA tape was also measured for the 25/30/45 silicone polyurea coatings following immersion in water at the various temperatures. For these experiments, the PSA tapes were applied within 15 minutes after removing the coatings from the water bath. Figure 13 shows how the initial (30-second dwell) peel force depends on the surface compositions of

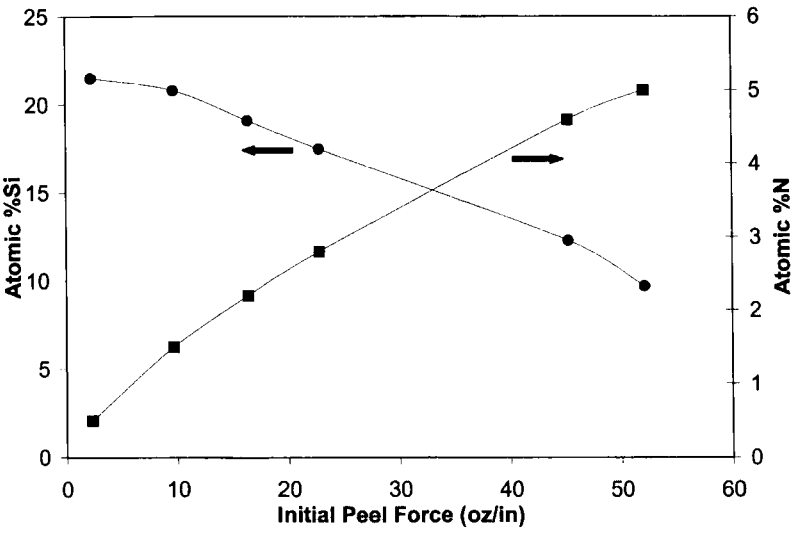

FIGURE 13 Initial peel force of the acidic acrylate PSA based tape peeled from the 25/30/45 silicone polyurea *versus* the XPS atomic% silicon and nitrogen, detected at a 15-degree takeoff angle, following water immersion of the silicone polyurea coating at temperatures between 21°C and 80°C.

nitrogen and silicon, as determined by XPS at a 15-degree takeoff angle. A large increase in the peel force is observed as the water immersion temperature is increased due to the higher extent of interfacial restructuring within the silicone polyurea. A good correlation is observed between the nitrogen or silicon concentration at the coating surface and the peel force of the PSA tape. Higher nitrogen levels indicate a higher concentration of the basic urea linkages at the interface with the acidic acrylate PSA, resulting in an increase in the acid-base interactions and an increase in the peel force.

CONCLUSIONS

In this paper, the bulk, surface and interfacial structures of a series of polyureas containing polydimethylsiloxane segments were examined. The siloxane segments were observed to form well-phase-separated spherical microdomains, while the matrix phase was comprised of a mixture of the polypropylene oxide soft segments and the hard

segments. The single glass transition temperature of the matrix phase increased systematically as the ratio of hard segment to polypropylene oxide soft segment increased. All of the silicone polyureas exhibited a thin 15 to 20 Å overlayer of the siloxane segments at their surface. The ability of the silicone polyurea surfaces to restructure upon contact with either water or an acid-functional acrylate pressure sensitive adhesive was also studied. The extent and rate of decrease in the receding water contact angle, as a function of water dwell time and temperature, was found to be related to the segmental mobility within the near-surface region of the silicone polyurea coatings. Silicone polyureas having higher hard segment content, and higher non-silicone matrix glass transition temperatures, were better able to maintain a high receding water contact angle, due to their lower segmental mobility. The observed increases in adhesion of the pressure sensitive adhesive, with increasing aging time and/or temperature, are attributed to an increase in the acid-base interactions between urea groups in the silicone polyurea and acrylic acid groups in the PSA. The initially low peel forces can be more readily maintained for the silicone polyureas having high hard segment contents, due to the reduced segmental mobility and reduced degree of interfacial restructuring within the silicone polyurea.

Acknowledgements

The author would like to acknowledge Teresa A. Kruger for DSC measurements, Dr. Diane B. Scott for dynamic tensile testing, Dr. Patricia J.A. Brandt and Scott D. Anderson for synthesis of the silicone polyureas, Dr. Alphonsus V. Pocius for assistance with surface analysis, Dr. Walter R. Romanko for assistance with inversion of the XPS angle-resolved data, and Dr. Charles M. Leir for many helpful discussions.

References

[1] Clark, D. T., Peeling, J. and O'Malley, J. M., *J. Polym. Sci., Polym. Chem. Ed.* **9**, 879 (1976).
[2] Schmitt, R. L., Gardella, J. A. Jr., Magill, J. H., Salvati, L. Jr. and Chin, R. L., *Macromol.* **18**, 2675 (1985).
[3] Tezuka, Y., Fukushima, A., Matsui, S. and Imai, K., *J. Coll. Interf. Sci.* **114**(1), 16 (1986).

[4] Patel, N. M., Dwight, D. W., Hedrick, J. L., Webster, D. C. and McGrath, J. E., *Macromol.* **21**, 2689 (1988).
[5] Tezuka, Y., Ono, T. and Imai, K., *J. Coll. Interf. Sci.* **136**(2), 408 (1990).
[6] Tezuka, Y., Kazama, H. and Imai, K., *J. Chem. Soc. Faraday Trans.* **87**(1), 147 (1991).
[7] Chen, X., Gardella, J. A. Jr. and Kumler, P. L., *Macromol.* **25**, 6621 (1992).
[8] Smith, S. D., Desimone, J. M., Huang, H., York, G., Dwight, D. W., Wilkes, G. L. and McGrath, J. E., *Macromol.* **25**, 2575 (1992).
[9] Chen, X., Lee, H. F. and Gardella, J. A. Jr., *Macromol.* **26**, 4601 (1993).
[10] Chen, X., Gardella, J. A. Jr., Ho, T. and Wynne, K. J., *Macromol.* **28**, 1635 (1995).
[11] Andrade, J. D., In: *Polymer Surface Dynamics* Andrade, J. D. Ed. (Plenum Press, New York, 1989).
[12] Holly, F. J. and Refojo, M. F., *J. Biomed. Res.* **9**, 315 (1975).
[13] Yasuda, H., Sharma, A. K. and Yasuda, T., *J. Polym. Sci.: Polym. Phys. Ed.* **19**, 1285 (1981).
[14] Lee, S. H. and Ruckenstein, E., *J. Coll. Interface Sci.* **120**, 529 (1987).
[15] Holmes-Farley, S. R., Reamey, R. H., Nuzzo, R., McCarthy, T. J. and Whitesides, G. M., *Langmuir* **3**, 799 (1987).
[16] Yasuda, T., Okuno, T., Yoshida, K. and Yasuda, H., *J. Polym. Sci.: Part B: Polym. Phys.* **26**, 1781 (1988).
[17] Ruckenstein, E. and Gourisankar, S. V., *J. Coll. Interface Sci.* **107**, 488 (1985).
[18] Cross, E. M. and McCarthy, T. J., *Macromol.* **23**, 3916 (1990).
[19] Lavielle, L. and Schultz, J., *J. Coll. Interface Sci.* **106**, 438 (1985).
[20] Teraya, T., Takahara, A. and Kajiyama, T., *Polymer* **31**, 1149 (1990).
[21] Tezuka, Y., Okabayashi, A. and Imai, K., *J. Coll. Int. Sci.* **141**(2), 586 (1991).
[22] Tezuka, Y., Yoshino, M. and Imai, K., *Langmuir* **7**, 2860 (1991).
[23] Lewis, K. B. and Ratner, B. D., *J. Coll. Int. Sci.* **159**, 77 (1993).
[24] Mori, H., Hirao, A., Nakahama, S. and Senshu, K., *Macromol.* **27**, 4093 (1994).
[25] Yasuda, T., Miyama, M. and Yasuda, H., *Langmuir* **10**, 583 (1994).
[26] Tezuka, Y. and Araki, A., *Langmuir* **10**, 1865 (1994).
[27] Yasuda, H., Okuno, T., Sawa, Y. and Yasuda, T., *Langmuir* **11**, 3255 (1995).
[28] Senshu, K., Yamashita, S., Mori, H., Ito, M., Hirao, A. and Nakahama, S., *Langmuir* **15**, 1754 (1999).
[29] Senshu, K., Kobayashi, M., Ikawa, N., Yamashita, S., Hirao, A. and Nakahama, S., *Langmuir* **15**, 1763 (1999).
[30] Kasemura, T., Takahashi, S., Nakane, N. and Maegawa, T., *Polymer* **37**(16), 3659 (1996).
[31] Kinning, D. J., *J. Adhesion* **60**, 249 (1997).
[32] Wang, J., Mao, G., Ober, C. K. and Kramer, E. J., *Macromol.* **30**, 1906 (1997).
[33] Magnani, A., Barbucci, R., Lewis, K. B., Leach-Scampavia, D. and Ratner, B. D., *J. Mater. Chem.* **5**(9), 1321 (1995).
[34] Park, D., Keszler, B., Galiatsatos, V., Kennedy, J. P. and Ratner, B. D., *Macromol.* **28**(8), 2595 (1995).
[35] Chen, J. H. and Ruckenstein, E., *J. Coll. Interface Sci.* **135**, 496 (1990).
[36] Deng, Z. and Schreiber, H. P., *J. Adhesion* **36**, 71 (1991).
[37] Pike, J., Ho, T. and Wynne, K. J., *Chem. Mater.* **8**, 856 (1996).
[38] Hoffman, J. J. and Leir, C. M., *Polymer International* **24**, 131 (1991).
[39] Briggs, D., In: *Encyclopedia of Polymer Science and Engineering* (*Surface Analysis*), **16** (John Wiley & Sons, New York, 1989), 399.
[40] Seah, M. P. and Dench, W. A., *Surf. Interface Analysis* **1**, 2 (1979).
[41] *Polymer Handbook*, 2nd edn., Brandrup, J. and Immergut, E. H. Eds. (Wiley-Interscience, New York, 1975).
[42] Wu, S., *Polymer Interface and Adhesion* (Marcel Dekker, New York, 1982).
[43] Tyler, B. J., Castner, D. G. and Ratner, B. D., *Surf. Interface Analysis* **14**, 443 (1989).
[44] Kajiyama, T., Tanaka, K. and Takahara, A., *Macromol.* **28**, 3482 (1995).